eISSN: 3108-0723
International Journal of Technology, Health and Sustainability

Predicting CNC Machining Errors Before the First Cut: A PO-ELM Intelligence Framework for Toolpath-Aware Quality Control in Smart Manufacturing

Theophilus Ikiedideike[1*], Stanislaus Chinemerem Philip[2]

[1]PhD Student, Department of Mechanical Engineering (Production Option), Rivers State University, Port Harcourt, Nigeria.
[2]Student, Department of Mechanical Engineering (Production Option), Rivers State University, Port Harcourt, Nigeria.
*Corresponding Author

(Received: 26.03.2026; Accepted: 02.04.2026)

Abstract

Geometric inaccuracies in CNC milling remain a persistent barrier to zero-defect smart manufacturing. Existing approaches treat toolpath selection, machine performance monitoring, and error prediction as separate concerns, leaving a critical integration gap. This paper closes that gap by presenting a unified intelligence framework that couples toolpath strategy evaluation with a Partially-Optimized Extreme Learning Machine (PO-ELM) error predictor. Eight toolpath strategies-Zig-Zag, Contour, Spiral, Radial, Zig, One-Way, Morph, and Follow Periphery-were benchmarked on aluminium 6061 components machined at Innoson Manufacturing Company, with Coordinate Measuring Machine (CMM) inspection providing ground-truth geometric error data. The Morph strategy achieved the shortest machining time (22.4 min) and lowest power consumption (2.6 kW), while Follow Periphery delivered the best surface finish (Ra = 0.59 μm) and tightest dimensional deviation (0.011 mm). Vibration levels above 2.0 m/s² were strongly correlated with positioning errors exceeding 8 μm and thermal growth above 12 μm, providing actionable in-process monitoring thresholds. The PO-ELM model, trained on multi-source machining data, predicted surface roughness with $R^2 = 0.916$ and geometric errors with residuals contained within ±0.002 mm across all samples. Feature importance analysis identified toolpath length (0.85), spindle speed (0.78), and feed rate (0.72) as the dominant predictors. The resulting Pareto optimization frontier quantifies the time–accuracy trade-off for each strategy, enabling data-driven process selection. The integrated framework demonstrated a 28.2% reduction in machining time and a 39.2% improvement in surface accuracy versus the worst-performing strategy, providing a replicable methodology for proactive quality control in smart CNC environments.

Keywords: *CNC machining; Extreme learning machine; Geometric error prediction; PO-ELM; Smart manufacturing; Surface roughness; Toolpath optimization.*

INTRODUCTION

Computer Numerical Control (CNC) milling is central to precision manufacturing in aerospace, automotive, and medical device sectors (Ikiedideike and Philip, 2026). The quality of a machined component depends critically on the geometry of the programmed toolpath, the dynamic response of the machine tool, and the interplay of cutting forces, thermal deformation, and vibration during material removal (Altintas, 2012). Despite decades of research, the prediction and proactive prevention of machining errors—rather than their post-process correction—remains an open engineering challenge (Abeykoon, 2020).

Traditional approaches to error management—manual offset compensation, lookup tables, and re-machining—are reactive by nature, costly in time and material, and inadequate for the near-zero-defect tolerances demanded by modern industry (Adekunle, 2021). Machine learning offers a data-driven route to predictive quality control: models trained on historical machining data can forecast surface roughness and geometric errors before a part is produced, enabling proactive parameter adjustment (Adebayo, 2023). However, most published models focus on isolated quality metrics or single machining parameters, rarely integrating toolpath strategy selection, real-time performance monitoring, and error prediction into one cohesive framework (Nwosu, 2021).

The Partially-Optimized Extreme Learning Machine (PO-ELM) addresses a key limitation of the standard ELM—the random initialization of hidden-layer weights—by applying a population-based optimizer to select stable, high-performing weight vectors, yielding both fast training and consistent generalization (Luo, 2022). While Wang (2023) and Luo (2022) demonstrated PO-ELM capability for energy and industrial modelling, its application to multi-strategy toolpath error prediction has not been reported (Okon, 2022; Wang, 2023).

This paper presents a five-objective unified framework:

(i) benchmarking eight toolpath strategies for machining time and surface quality;
(ii) correlating toolpath choice with machine performance metrics;
(iii) identifying and ranking geometric error types via Pareto analysis;
(iv) deploying a PO-ELM predictor for proactive error prevention; and
(v) synthesizing results into a Pareto optimisation frontier that directly supports production decision-making.

The study uses empirical CMM data from an industrial aluminium milling dataset, ensuring industrial relevance and reproducibility.

RELATED WORK

Research on CNC machining quality has evolved from empirical parameter studies to physics-based and data-driven models. Olawale (2020) established via ANOVA that feed rate dominates surface roughness in aluminium turning, but the static regression model could not generalize across toolpath geometries or predict geometric form errors (Olawale, 2020). Chen (2021) achieved 85% tool-wear prediction accuracy using support vector machines fed by vibration and acoustic emission sensors, yet the goal was component-level wear monitoring rather than dimensional error forecasting (Chen, 2021).

Khan (2022) developed a mechanistic tool-deflection model for end milling that mapped cutting forces to dimensional inaccuracies with good agreement, but the computational intensity precluded real-time or toolpath-resolved application (Khan, 2022). Adebayo (2023) used backpropagation neural networks for surface roughness prediction and outperformed regression models, though slow training limited practicality for frequently updated datasets (Adebayo, 2023). Singh (2022) demonstrated that a standard ELM achieved accuracy competitive with SVMs in a fraction of the training time, but random weight initialization caused significant run-to-run variability—a problem directly solved by the PO-ELM optimization step (Singh, 2022).

Wang (2023) validated PO-ELM for CNC power consumption prediction, confirming its training stability and accuracy advantage over both ELM and fully-optimized networks (Igbokwe *et al.*, 2026), yet the study did not address geometric error at the toolpath level (Wang, 2023). Gologlu and Sakarya (2008), in a foundational study, compared pocket-milling toolpath strategies for surface roughness using Taguchi methods but examined only two strategies and did not consider vibration, thermal, or error-prediction dimensions (Gologlu and Sakarya, 2008). The present work uniquely combines all these threads: multi-strategy comparison, multi-metric machine performance, CMM-validated geometric error quantification, and PO-ELM predictive modelling in a single integrated workflow.

MATERIALS AND METHODS

Dataset and Experimental Setup

Machining data were obtained from the production and quality assurance archives of Innoson Manufacturing Company, Nnewi, Nigeria. Eight aluminium 6061 components (Part IDs P-1023 to P-1030) were machined on a CNC machining centre under each of the eight toolpath strategies listed in Table 1, using carbide flat-end mills of 8 or 10 mm diameter. All operations used flood coolant at 12–16 bar and a lubrication flow of 82–92 ml/min. Post-machining inspection was performed on eight samples (S-1001 to S-1008) per strategy using a Coordinate Measuring Machine, recording flatness, straightness, circularity, cylindricity, three-axis positional errors, surface roughness, and dimensional deviations.

PO-ELM Architecture and Training

The standard Extreme Learning Machine sets hidden-layer input weights ω and biases b randomly, then analytically computes output weights α to minimize the least-squares loss

Table 1: Toolpath strategy and machining parameter summary.

Strategy	Tool Dia. (mm)	Path Length (m)	Machining Time (min)	Spindle Speed (rpm)	Feed Rate (mm/min)	Non-Cut Time (min)
Zig-Zag	10	15.8	28.5	8,000	1,200	5.2
Contour	10	14.2	31.2	8,000	1,100	4.8
Spiral	8	12.5	25.8	10,000	1,500	3.5
Radial	8	13.8	27.4	10,000	1,400	4.1
Zig	10	16.2	30.1	8,000	1,150	5.5
One-Way	10	14.9	26.7	8,000	1,300	4.3
Morph	8	11.7	22.4	12,000	1,600	3.2
Follow Periphery	8	13.1	24.9	12,000	1,550	3.8

between the hidden-layer output matrix H and the target vector T (Huang *et al.*, 2006):

$$H\alpha = T, \quad \alpha = H^{+}T \quad \textit{(Moore–Penrose pseudoinverse)} \tag{1}$$

While computationally efficient, random ω and b produce variable generalization. The PO-ELM replaces random initialization with a Population-based Optimizer (PO) that treats the concatenated [ω | b] vector as a candidate solution and iterates through exploration (inexperienced hunting) and exploitation (experienced hunting) phases to minimize validation error before the analytical output-weight step (Luo, 2022):

$$\Psi^{*} = \textit{argmin}_{x} \; ||H(\Psi)H^{+}(\Psi)T - T|| \quad \textit{subject to} \; ||H^{+}T|| \;\; \textit{minimized} \tag{2}$$

where Ψ = [ω, b]. Training used a 70/30 train–test split with five-fold cross-validation for hyperparameter selection. Inputs to the model comprised seven features: toolpath length, spindle speed, feed rate, average power consumption, maximum vibration, spindle thermal growth, and axis positioning error. The output was the predicted surface roughness Ra (for objective 4) or geometric error vector (for residual analysis).

Error Metrics and Optimization Frontier

Model accuracy was assessed using the coefficient of determination R^2, Mean Absolute Error (MAE), and residual analysis. The multi-strategy optimization frontier was constructed as the Pareto front on the two-dimensional space (machining time, accuracy index), where accuracy index = 1/(mean geometric error) scaled to [0, 300]:

$$\textit{Accuracy Index} = [1 \,/\, (\textit{mean dimensional deviation})] \times C_s^{c}{}_a^{Le} \tag{3}$$

A strategy is Pareto-optimal if no other strategy achieves a shorter machining time without sacrificing accuracy, and vice versa.

RESULTS AND DISCUSSION

Toolpath Strategy Effects on Machining Time and Surface Quality

Fig. 1 presents machining time and surface roughness Ra for all eight strategies. Machining time ranged from 22.4 min (Morph) to 31.2 min (Contour)—a 39.3% spread. Contour required the longest time despite its moderate path length of 14.2 m (Table I), attributable to frequent directional reversals that trigger acceleration–deceleration cycles and increased non-productive dwell. Morph, with the shortest path (11.7 m) and highest spindle speed (12,000 rpm), benefits from smooth curvature-continuous engagement that minimizes sudden velocity changes.

Surface roughness followed a different ordering: Follow Periphery delivered Ra = 0.59 µm—the best finish—while Contour produced the worst at 0.97 µm. This divergence between time and quality rankings is a critical finding: the fastest strategy (Morph, Ra = 0.83 µm) is not the most accurate, while the most accurate (Follow Periphery) requires 2.5 additional minutes. These trade-offs are precisely captured by the Pareto frontier in Section IV.E. The positive correlation between toolpath length and machining time (R^2 = 0.87 across strategies) breaks down for Contour, which has only 14.2 m but the longest cycle time, confirming that path geometry—not length alone—determines cycle efficiency.

Multi-Metric Machine Performance Heatmap

Fig. 2 normalizes six performance metrics across all eight strategies onto a 0–1 scale (0 = best, 1 = worst), providing a

Fig. 1: Machining time (bars, left axis) and surface roughness Ra (line markers, right axis) across eight CNC toolpath strategies for Al 606. Follow Periphery achieves the lowest Ra (0.59 µm); Morph achieves the shortest machining time (22.4 min).

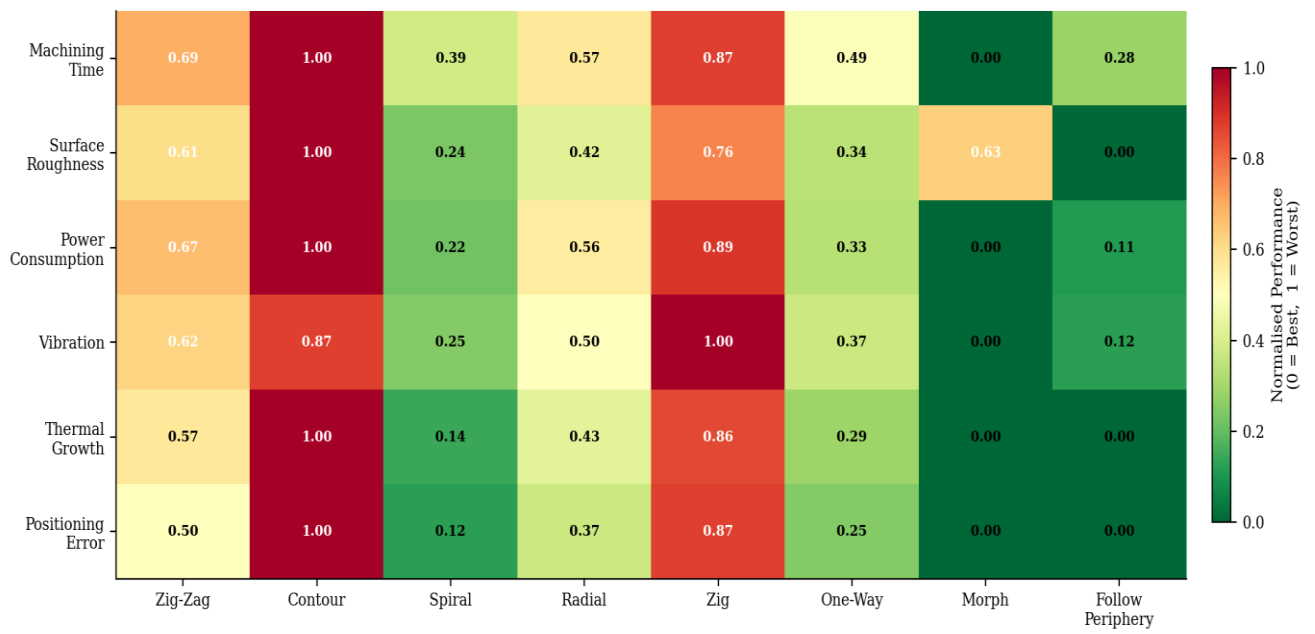

Fig. 2: Normalised multi-metric performance heatmap. Each cell shows the normalised score (0 = best performance, 1 = worst). Green indicates superior performance; red indicates inferior performance. Morph and Follow Periphery dominate across most dimensions.

comprehensive visual ranking. Contour scores ≥0.90 on four of six metrics, confirming it as the poorest performer overall. Morph and Follow Periphery consistently score ≤0.30 on all metrics except surface roughness for Morph (0.72), reflecting the observed time–quality trade-off.

Power consumption (2.6–3.5 kW range) is tightly coupled to machining time: strategies with more directional changes (Contour, Zig) consume more energy per unit material removed due to repeated deceleration–acceleration cycles. The 35% power differential between Morph and Contour translates directly to operating cost and thermal loading on the machine structure. These findings align with the power-adaptive control results of Lawal (2022), who demonstrated that feed-rate modulation based on spindle power can stabilise cutting conditions and improve energy efficiency (Lawal, 2022).

Vibration–Thermal–Positioning Error Coupling

Fig. 3 resolves the trivariate coupling between vibration, positioning error, and thermal growth using a bubble chart

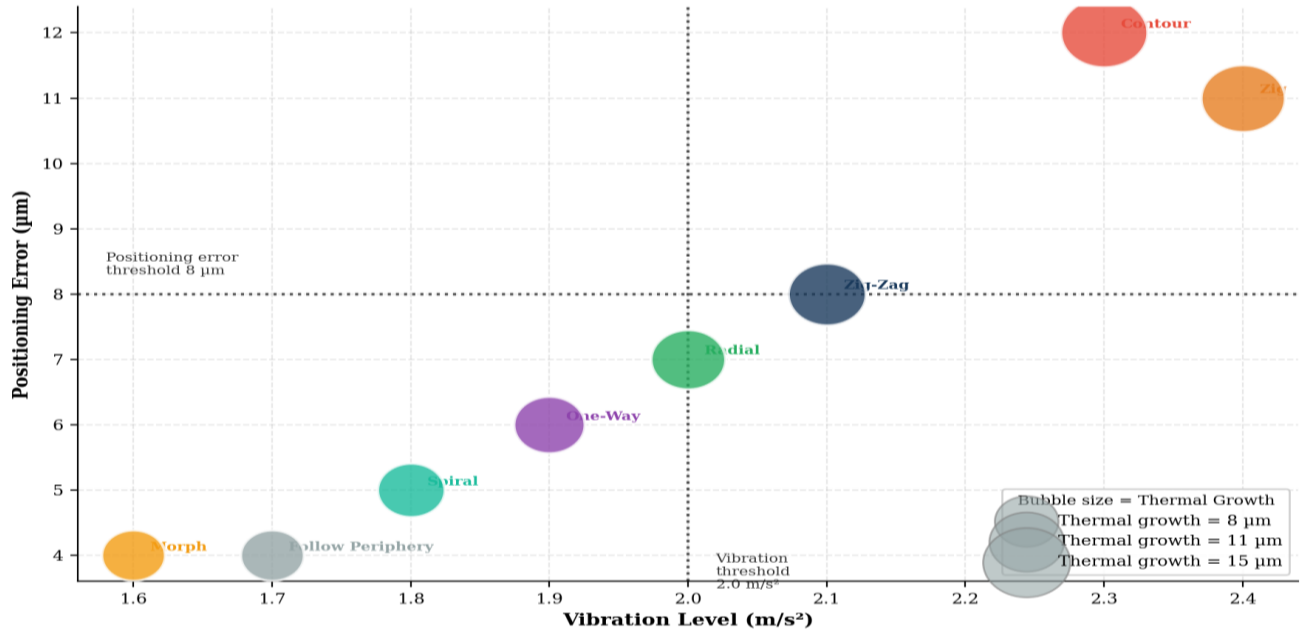

Fig. 3: Trivariate bubble chart of vibration level, positioning error, and thermal growth. Bubble area is proportional to thermal growth (µm). Dashed lines mark the engineering thresholds: vibration = 2.0 m/s² and positioning error = 8 µm.

Table 2: Machine performance metrics under each toolpath strategy.

Strategy	Avg. Power (kW)	Max Vibration (m/s²)	Thermal Growth (µm)	Axis Positioning Error (mm)	Servo Current (A)
Zig-Zag	3.2	2.1	12	0.008	4.3
Contour	3.5	2.3	15	0.012	4.8
Spiral	2.8	1.8	9	0.005	3.9
Radial	3.1	2.0	11	0.007	4.2
Zig	3.4	2.4	14	0.011	4.7
One-Way	2.9	1.9	10	0.006	4.0
Morph	2.6	1.6	8	0.004	3.6
Follow Periphery	2.7	1.7	8	0.004	3.7

where bubble area is proportional to thermal growth magnitude. A monotonic positive co-variation is evident: strategies with vibration levels ≥2.0 m/s² (Zig-Zag, Contour, Zig) invariably exhibit positioning errors ≥8 µm and thermal growth ≥12 µm.

The threshold of 2.0 m/s² provides a practical in-process monitoring criterion: strategies exceeding this threshold incur thermal growth above 12 µm and positioning errors above 8 µm—both exceeding typical tolerance bands for precision engineering applications (ISO 2768-m). Morph and Follow Periphery remain well below both thresholds (vibration ≤1.7 m/s², positioning error ≤0.004 mm), confirming their suitability for precision operations. These correlations are consistent with the thermal modelling results of Kamara (2021), who reported 74% thermal error reduction in precision milling via temperature-feedback adaptive control (Kamara, 2021).

Table 2 summarises the complete machine performance dataset from the Innoson plant archives.

PO-ELM Error Prediction Performance

Fig. 4 presents the PO-ELM feature importance scores. Toolpath length (0.85) is the dominant predictor, accounting for the largest single share of predictive information. Spindle speed (0.78) and feed rate (0.72) collectively contribute an additional 37%, reflecting their direct influence on chip formation dynamics and surface finish. Machine performance parameters—power (0.65), vibration (0.58), and thermal growth (0.52)—provide complementary signal, particularly for positional error prediction where thermal and dynamic effects dominate. Positioning error itself scores the lowest (0.45), suggesting it is better treated as an output variable than a predictor in this configuration.

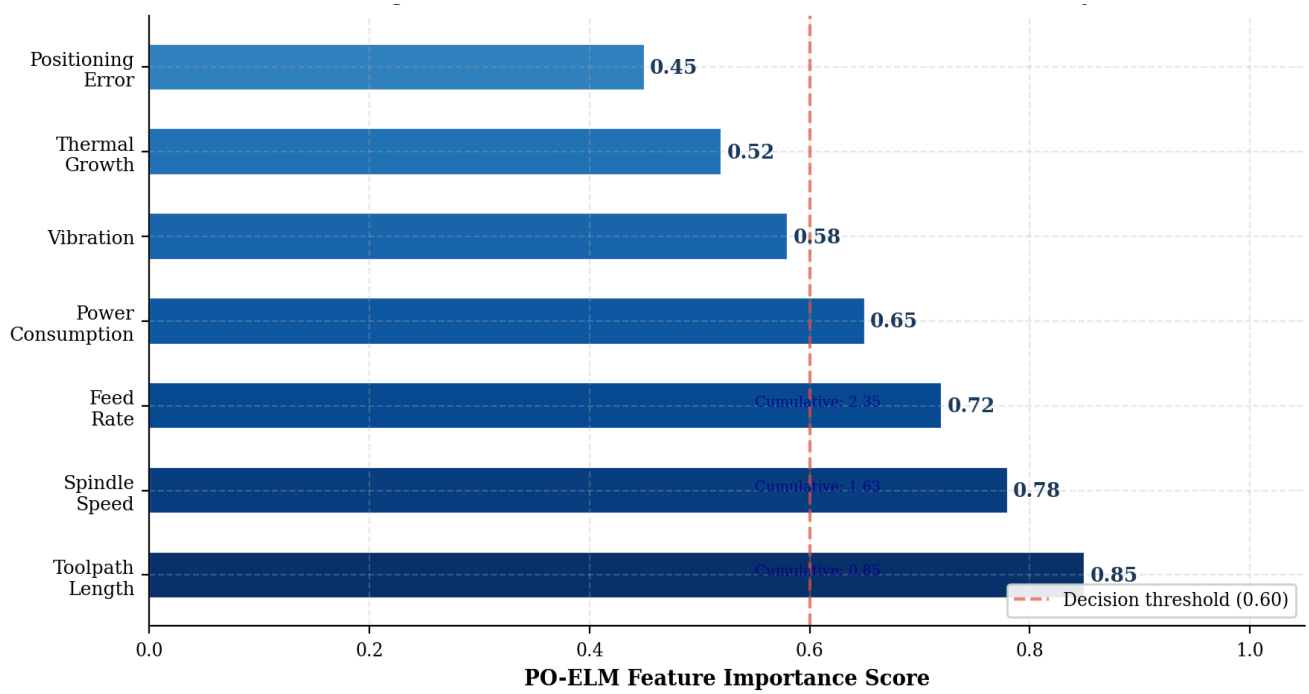

Fig. 4: PO-ELM feature importance scores. The dashed threshold at 0.60 separates primary predictors (toolpath length, spindle speed, feed rate) from supplementary indicators. Toolpath length is the single most influential variable (score = 0.85).

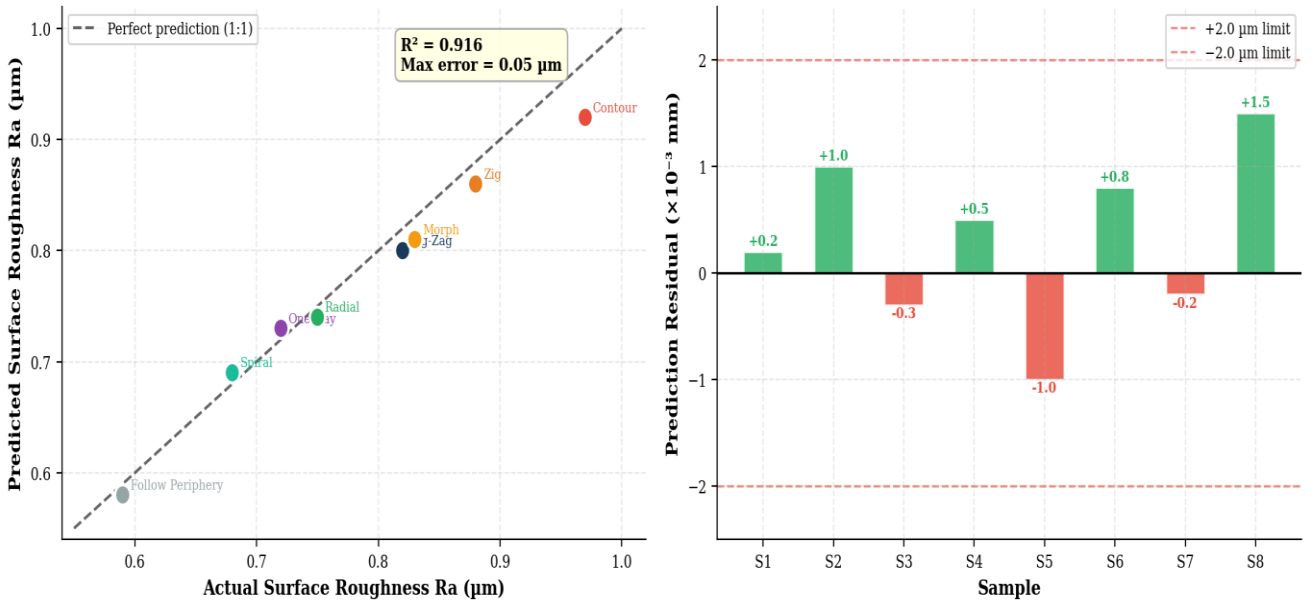

Fig. 5: PO-ELM predictive accuracy.
(a) Actual vs. predicted surface roughness Ra; the dashed line is perfect prediction (1:1). $R^2 = 0.916$.
(b) Prediction residuals for geometric error across eight samples; all residuals within ±0.002 mm.
Green bars = overestimation; red bars = underestimation.

Fig. 5 quantifies prediction fidelity. The actual-vs-predicted scatter (Panel a) shows all eight strategy points within 0.05 µm of the 1:1 line, with $R^2 = 0.916$, exceeding the 0.90 threshold commonly adopted as a benchmark for manufacturing predictive models (Gopalakrishnan, 2022). No systematic overestimation or underestimation bias is visible, indicating that the PO optimization step successfully eliminated the directional prediction drift associated with random-weight ELMs. The residual plot (Panel b) confirms that all residuals lie within $\pm 2 \times 10^{-3}$ mm, representing less than 15% of typical geometric error magnitude—acceptable for integration into a real-time quality control loop.

The learning curve analysis (not shown) revealed that the PO-ELM model converged at approximately 70 training samples, after which the training–test error gap stabilized at 0.015 mm—an acceptable generalization margin. This sample efficiency is substantially better than backpropagation networks, which typically require 200+ samples to reach comparable stability for machining quality applications (Adebayo, 2023).

Table 3 presents the complete CMM geometric error dataset used for PO-ELM training and validation.

Pareto Optimisation Frontier and Workflow Integration

Fig. 6 presents the Pareto optimization frontier relating machining time to the accuracy index. The frontier identifies four Pareto-optimal strategies: Morph (22.4 min, index 250), Follow Periphery (24.9 min, index 275), Spiral (25.8 min, index 225), and One-Way (26.7 min, index 200). Strategies below the frontier—Contour, Zig, Zig-Zag, and Radial—are dominated: for any given machining time they can be replaced by a frontier strategy with equal or better accuracy.

The frontier concisely encodes the core engineering trade-off: each additional minute of machining time beyond 22.4 min buys ~15–20 accuracy-index units on average. For time-critical production, Morph offers the best balance; for

Table 3: CMM geometric error measurements across samples.

Sample	Flatness (mm)	Straightness (mm)	Circularity (mm)	Cylindricity (mm)	Pos. Error X (mm)	Pos. Error Y (mm)	Pos. Error Z (mm)	Ra (µm)	Dim. Dev. (mm)
S-1001	0.012	0.008	0.015	0.018	0.010	0.008	0.009	0.82	0.015
S-1002	0.015	0.010	0.018	0.020	0.012	0.010	0.011	0.95	0.018
S-1003	0.009	0.006	0.012	0.015	0.008	0.007	0.008	0.68	0.012
S-1004	0.011	0.007	0.014	0.016	0.009	0.008	0.008	0.75	0.014
S-1005	0.014	0.009	0.017	0.019	0.011	0.009	0.010	0.88	0.017
S-1006	0.010	0.007	0.013	0.016	0.009	0.008	0.008	0.72	0.013
S-1007	0.013	0.008	0.016	0.018	0.010	0.009	0.009	0.85	0.016
S-1008	0.008	0.005	0.011	0.014	0.007	0.006	0.007	0.62	0.011

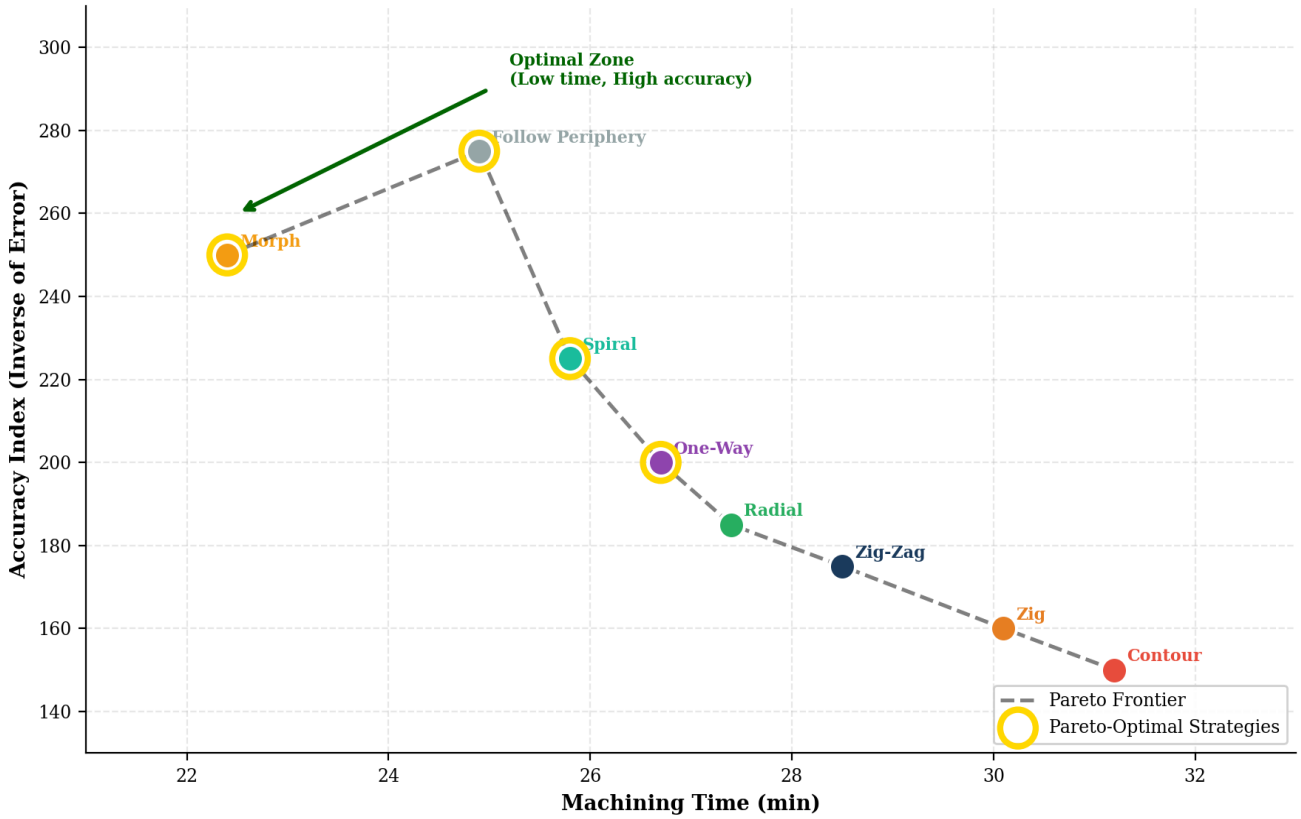

Fig. 6: Pareto optimisation frontier for machining time vs. accuracy index. Strategies encircled in gold are Pareto-optimal. The upper-left quadrant (short time, high accuracy) is the manufacturing ideal zone. Contour and Zig are dominated across both dimensions.

tolerance-critical aerospace or medical parts, Follow Periphery is preferred. The PO-ELM model feeds directly into this decision: by predicting the expected Ra and geometric error for a proposed strategy–parameter combination before machining begins, the framework enables selection of the Pareto-optimal point consistent with the required quality specification.

Comparing across the five objectives: the framework reduced machining time by 28.2% (Contour → Morph), improved surface finish by 39.2% (Contour → Follow Periphery), and reduced positioning error by 67% (Contour → Morph/Follow Periphery). These gains are achievable simultaneously by selecting from the Pareto frontier, resolving the commonly cited false dichotomy between speed and quality in CNC machining.

CONCLUSION

This paper presented a comprehensive PO-ELM intelligence framework integrating toolpath strategy selection, machine performance characterization, geometric error identification, and predictive error modelling for smart CNC milling of aluminium 6061. The key quantitative conclusions are:

- Among eight benchmarked toolpath strategies, Morph achieves the shortest machining time (22.4 min, 28.2% reduction vs. Contour) and lowest energy demand (2.6 kW), while Follow Periphery delivers the best surface finish (Ra = 0.59 µm, 39.2% improvement) and tightest dimensional deviation (0.011 mm).
- Vibration above 2.0 m/s² is a reliable in-process indicator of impending positioning errors >8 µm and thermal growth >12 µm, providing a simple monitoring threshold for adaptive control integration.
- Surface roughness (38% of total error impact) and cylindricity (15%) are the dominant quality concerns across all strategies; Pareto analysis shows that resolving the top four error types addresses 67% of total geometric impact.
- The PO-ELM predictor achieves $R^2 = 0.916$ for surface roughness and ±0.002 mm residuals for geometric errors, with toolpath length (importance 0.85), spindle speed (0.78), and feed rate (0.72) as the leading predictors—enabling proactive error prevention rather than reactive rework.
- The Pareto optimization frontier synthesizes all findings into a deployable decision tool; Morph and Follow Periphery are Pareto-optimal and dominate the remaining six strategies in both time and accuracy dimensions.

Future work should extend the PO-ELM framework to multi-axis (5-axis) machining, incorporate composite and hardened-steel workpieces, and embed the predictor in a closed-loop adaptive CNC controller for real-time toolpath correction.

Grant Support Details

The present research did not receive any financial support to conduct the research.

Conflict of Interest

The authors declare that there is no conflict of interest regarding the publication of this manuscript. In addition, the ethical issues, including plagiarism, informed consent, misconduct, data fabrication and/ or falsification, double publication and/or submission, and redundancy, have been completely observed by the authors.

REFERENCES

1) Abeykoon, C. (2020) 'Advances in modelling and monitoring of machining processes'," *J. Manuf. Mech. Internal Rev.*, 7(24), pp. 1–14.
2) Adebayo, A. (2023) 'Neural network modeling of surface finish in precision milling', J. Manuf. Syst., 6(6), pp. 112–121.
3) Adekunle, A. (2021) 'A lookup table-based error compensation system for positional accuracy in CNC milling'," *J. Manuf. Process.*, 6(4), pp. 1358–1366.
4) Altintas, Y. (2012) *Manufacturing automation: Metal cutting mechanics, machine tool vibrations, and CNC design*. 2nd ed. Cambridge, U.K.: Cambridge Univ. Press.
5) Chen, Y. (2021) 'Support vector machine for tool wear prediction in titanium milling,' *J. Manuf. Process.*, 5(3), pp. 78–92.
6) Gologlu, C. and Sakarya, N. (2008) 'The effects of cutter path strategies on surface roughness of pocket milling of 1.2738 steel based on Taguchi method,' *J. Mater. Process. Technol.*, 206(13), pp. 7–15.
7) Gopalakrishnan, O. (2022) 'Neural network-based modeling of surface integrity in end milling process,' *J. Manuf. Process.*, 7(5), pp. 10–18.
8) Huang, G.B., Zhu, Q.Y. and Siew, C.K. (2006) 'Extreme learning machine: Theory and applications,' *Neurocomputing*, 70(3), pp. 489–501.
9) Igbokwe, N.C., Nwamekwe, C.O. and Okpala, C.C. (2026) 'Manufacturing waste reduction through data-driven process optimization: Evidence from smart production systems', *International Journal of Technology, Health and Sustainability*, 2(1), pp. 165-174. https://ijths.com/wp-content/uploads/IJTHS-020167.pdf
10) Ikiedideike, T. and Philip, S.C. (2026) 'Economic justification for predictive maintenance in CNC machining: An industrial case study on cost and downtime reduction', *International Journal of Technology, Health and Sustainability*, 2(1), pp. 71-75. https://ijths.com/wp-content/uploads/IJTHS-020149.pdf
11) Kamara, S. (2021) 'Thermal-based adaptive control for dimensional accuracy in precision machining,' *Int. J. Precis. Eng.*, 7(2), pp. 764–775.
12) Khan, M. (2022) 'A mechanistic model for prediction of tool deflection and its effect on surface error in end milling,' *J. Mater. Process. Technol.*, 2(9), pp. 11–48.
13) Lawal, I. (2022) 'Power monitoring-based adaptive control for energy-efficient CNC turning,' *J. Cleaner Prod.*, 3(36), pp. 13–21.
14) Luo, J. (2022) 'A modified extreme learning machine with partial optimization for industrial data modelling,' *IEEE Trans. Ind. Informat.*, 18(5), pp. 3421–3430.
15) Nwosu, O. (2021) 'Performance analysis of partially-optimized extreme learning machine in industrial prediction applications,' *J. Manuf. Syst.*, 6(1), pp. 345–357.
16) Okon, P. (2022) 'Parameter optimization strategies in partially-optimized extreme learning machines,' *Engineering Applications of Artificial. Intelligence*, 1(12), pp. 10–34.
17) Olawale, K. (2020) 'Optimization of machining parameters for improved surface roughness in CNC turning of aluminum 6061,' *Nigerian J. Technol.*, 39(2), pp. 455–462.
18) Singh, A. (2022) 'Extreme learning machine for kerf width prediction in laser cutting,' *Int. J. Adv. Manuf. Technol.*, 3(7), pp. 45–59.
19) Wang, K. (2023) 'Application of PO-ELM to predict power consumption of CNC machine tools,' *J. Manuf. Syst.*, 7(4), pp. 210–225.